Nanocomposites Derived from Sulfonated Poly(butylene terephthalate)

Bret J. Chisholm,*,† Robert B. Moore,*,‡ Grant Barber,‡ Farid Khouri,† Anne Hempstead,† Michael Larsen,† Eric Olson,† Jim Kelley,† Gary Balch,† and Joel Caraher†

GE Corporate Research and Development, One Research Circle, Niskayuna, New York 12309, and Department of Polymer Science, The University of Southern Mississippi, PO Box 10076, Hattiesburg, Mississippi 39406-0076

Received December 21, 2001

ABSTRACT: The effect of sodium sulfonate functionalization of poly(butylene terephthalate) (PBT) on the properties of PBT/montmorillonite composites was studied. The results of the study clearly showed that organic modification of montmorillonite clay coupled with the modification of PBT with low levels (1.0−5.0 mol %) of $-SO_3Na$ groups results in the production of highly exfoliated nanocomposites by a simple extrusion process. With regard to the effect of $-SO_3Na$ content, as little as 1.0 mol % $-SO_3Na$ groups was needed to achieve considerable exfoliation of R_4N^+ montmorillonite. Although the degree of exfoliation was not observed to be strongly dependent on $-SO_3Na$ content, mechanical properties such as Young's modulus and high-temperature storage moduli at temperatures above T_g increased with increasing $-SO_3Na$ content. These enhancements in mechanical properties produced by a higher $-SO_3Na$ content were due to an increase in the number of interactions between the clay particles and the matrix via electrostatic interactions involving the $-SO_3Na$ groups.

Introduction

Nanocomposites refer to solid, multiphase materials in which at least one dimension of a dispersed phase is in the nanometer range, typically 1−20 nm. Polymeric, intercalation-type nanocomposites have been the subject of extensive research in both academia and industry over the past decade.[1−4] Much of the work in this area has been focused on polymeric nanocomposites derived from layered silicates such as montmorillonite. Examples of polymer matrices that have been utilized for the production of montmorillonite-containing nanocomposites include nylon-6,[5−8] polyimide,[9] polycaprolactone,[10,11] unsaturated polyesters,[12,13] epoxides,[14,15] and poly(dimethylsiloxane).[16,17] Polymer nanocomposites comprised of a semicrystalline polymer matrix are particularly attractive due to the dramatic improvement in heat distortion temperature and modulus provided by the nanoparticle reinforcement and the high flow character inherent to most commodity semicrystalline thermoplastics such as nylon-6, nylon-6,6, polybutylene terephthalate, poly(ethylene terephthalate), polypropylene, polyethylene, etc. Because of these desirable characteristics, semicrystalline polymer nanocomposites have been shown to be well suited for application as injection moldable thermoplastics.

Toyota was the first company to develop and commercialize polymer nanocomposites of this type. Their materials were based on nylon-6 as the polymer matrix. The process for producing the nanocomposites consisted of (1) organically modifying sodium montmorillonite by exchanging the sodium ions with an amino acid salt, (2) isolating the modified clay, and (3) polymerizing caprolactam in the presence of the modified clay.[6] With this process, the ion exchange between sodium cations and the ammonium cations increases the spacing between the silicate layers and makes the galleries between the layers more organophilic, facilitating intercalation of the clay with caprolactam. Upon polymerization of the caprolactam, which is initiated by carboxylic acid groups on the ammonium cations, the silicate layers are forced apart by the growing polymer chains creating the nanocomposite. With this process, polymer chains are tethered to the surface of the silicate reinforcement through ionic interactions between the negatively charged silicate surface and the positively charged ammonium cation on the end of the polymer chain.

Because of the charged nature of the aluminosilicate surfaces of montmorillonite clay, it has become of interest to determine the effect ionic groups present in a semicrystalline polymer would have on the morphology of montmorillonite composites. The semicrystalline, ion-containing polymer chosen for this investigation was sulfonated poly(butylene terephthalate).

Poly(butylene terephthalate) (PBT) is an important commercially available engineering thermoplastic for injection molding applications due to its excellent processability and mechanical properties. Ion-containing poly(butylene terephthalate) copolymers can be readily produced by the melt copolymerization of dimethyl terephthalate, dimethyl-5-sodiosulfoisophthalate, and 1,4-butanediol, as shown in Figure 1. Since the level of sodium sulfonate ($-SO_3Na$) groups in the copolymers under investigation was 10 mol % or less, the copolymers fall into the category of ion-containing polymers referred to as ionomers. As a result, the sulfonated poly(butylene terephthalate) copolymers have been referred to as PBT-ionomers.

The rheological and solid-state properties of the PBT-ionomers suggest that the $-SO_3Na$ groups aggregate together to form small ionic domains.[18,19] Because of the ionic nature of the $-SO_3Na$ groups and the expected insolubility of the $-SO_3Na$ groups in the polyester matrix, it was thought that the presence of the $-SO_3Na$ groups may provide a thermodynamic driving force for the production of nanocomposites derived from montmorillonite clays. Combining a PBT-ionomer with a montmorillonite clay may result in exfoliation of the

† GE Corporate Research and Development.
‡ The University of Southern Mississippi.
* To whom correspondence should be addressed.

10.1021/ma012224n CCC: $22.00
Published on Web 06/07/2002

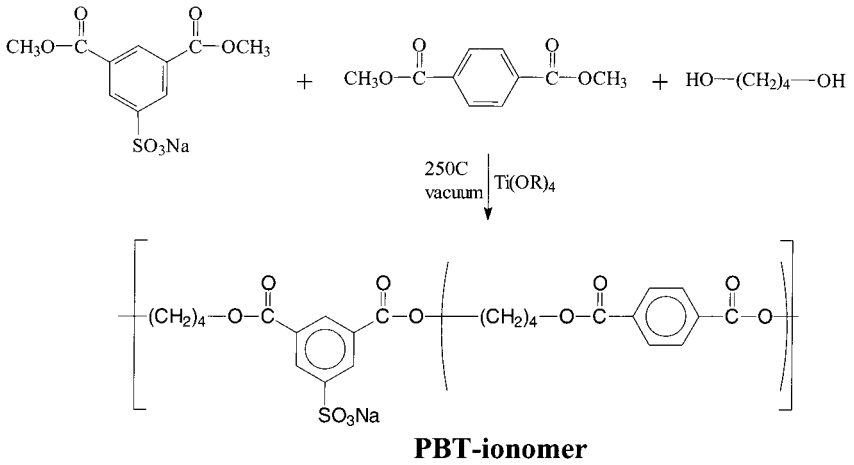

Figure 1. Synthesis of sulfonated poly(butylene terephthalate) copolymers (PBT-ionomers).

clay due to favorable electrostatic interactions between the charged surfaces of the silicate clay particles and the $-SO_3Na$ groups of the PBT-ionomer.

Experimental Section

Materials. PBT-ionomers were prepared by the melt polymerization of dimethyl terephthalate, dimethyl-5-sodiosulfoisophthalate, and 1,4-butanediol. A representative polymerization procedure is as follows: 125.9 lbs (294.1 mol) of dimethylterephthalate (DMT), 5.94 lbs (9.10 mol) of dimethyl-5-sodiosulfoisophthalate (DMSIP), 100.1 lbs (503.8 mol) of 1,4-butanediol, and 43 mL (0.15 mol) of tetraisopropyl titanate were charged to a 40CV Helicone reactor which was preheated to 130 °C. The monomer mixture was then heated to 225 °C at a rate of 1.5 °C/min under atmospheric pressure and most of the methanol byproduct removed by distillation. The mixture was then subjected to a gradual reduction in pressure at a rate of 20 mmHg/min while the temperature was simultaneously increased to 250 °C at a rate of 1.5 °C/min. After 132 min under vacuum, the batch was released from the reactor and chopped into granules.

The poly(butylene terephthalate) (PBT) was Valox 315 from GE Plastics. The ionic content of the ionomer is based on the mole percent of DMSIP present in the copolymer. The example polymerization procedure detailed above was for the production of the 3.0 mol % PBT-ionomer containing 3 mol of DMSIP to 97 mol of DMT, and the diol was 100% 1,4-butanediol. Sodium montmorillonite (Na^+ montmorillonite) was Kunipia F, which is a highly purified grade from Kunimine Industries. The organically modified montmorillonite (R_4N^+ montmorillonite) was Claytone HY from Southern Clay Products. The organic cation loading of the Claytone HY was 125 mequiv/100 g of clay. According to product literature, this organoclay is prepared by reacting a dimethyldihydrogenatedtallow alkyl quaternary ammonium counterion with the clay; the reaction results in exchange of the sodium ions with alkylammonium ions. The chemical composition of the hydrogenated tallow units consists of ca. 65% C18, ca. 30% C16, and ca. 5% C14 chains.

Melt Processing. All blends were extruded using a 20 mm WE twin screw extruder using a screw speed of 400 rpm and a barrel temperature setting of 250 °C. Mixtures for extrusion were prepared by shaking powders of the polymers with the clay in a 1 gal glass jar. The mixtures were used without drying before extrusion.

Molded parts for testing were produced by injection molding with a 30 ton Engel injection molding machine using a barrel temperature setting of 250 °C, mold temperature of 60 °C, cooling time of 22 s, hold time of 8 s, and injection speed of 2.2 in./s.

Characterization. Small-angle X-ray scattering (SAXS) data were obtained in the transmission mode using a Siemens XPD-700P polymer diffraction system equipped with a two-dimensional, position-sensitive area detector. The sample-to-detector distance was set at 49 cm, which yielded an angular scan from 1° to 6° (2θ). Thin samples were cut from the center of injection-molded tensile specimens, and the X-ray beam was directed through the center of the cross section and parallel to the long axis of the tensile specimen (*Z*-axis) as shown in Figure 2. The two-dimensional scattering patterns were analyzed using the GADDS software package and integrated radially, after background subtraction, to obtain intensity vs scattering angle 2θ plots. Using a 2-dimensional position-sensitive detector, 2-D scattering profiles were obtained for the purpose of evaluating the potential for preferential orientation of the clay platelets in the injected-molded samples. For all samples, the 2-D data were analyzed by performing an azimuthal integration across the scattering profiles from $\chi = 0°$ to 180° at a set 2θ position (band from 1.8° to 2.8°, 2θ). The samples were mounted in the instrument such that the azimuthal angle of 90° corresponds to scattering along the *X*-axis (i.e., in a direction normal to the flat surface of the tensile specimen).

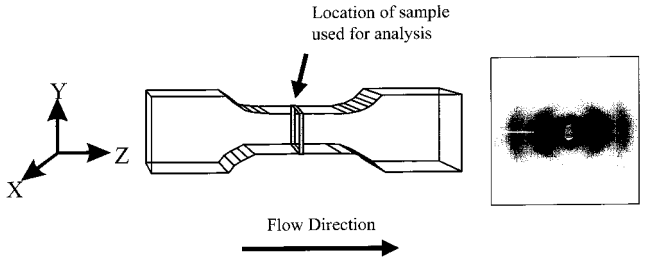

Figure 2. Positioning of X-ray beam to sample for SAXS experiments.

The morphology of the composites produced was investigated using transmission electron microscopy (TEM) employing a Philips CM100 microscope operated at 100 kV. Materials were prepared by ultramicrotomy performed at room temperature. Specimen blocks were extracted from injection-molded tensile specimens. Thin sections (typically <100 nm thick) sampled from the center of the specimen through the thickness. Images were processed and feature attributes were quantified using standard imaging software (Image Pro Plus). Digital TEM images for the measurement of *mean free path* were processed using Clemex Vision Image Analysis Software. The parameter *mean free path* is the 3-dimensional distance between features using stereological formulas.

Mechanical Properties. Young's modulus was determined on ASTM type IV tensile specimens using an Instron Universal Testing Machine model 4505.

Dynamic mechanical analysis (DMA) was conducted on specimens cut from the center of tensile bars using a Rheometrics Dynamic spectrometer model 7700 using a torsion rectangular fixture, heating rate of 2 °C/min, and a frequency of 10 rad/s.

Thermal Properties. Thermal analysis of the polymers and the respective composites were performed using a Perkin-Elmer DSC 7, which was calibrated using both indium and zinc standards. All samples (10 ± 1 mg) were cut from the center portion of injection-molded parts. Prior to analysis, the samples were heated to the melt (i.e., 280 °C) for a period of 4 min to normalize the thermal history. The samples were then quenched at a cooling rate of −200 °C/min to the isothermal crystallization temperature of 206 °C, and the crystallization exotherm was monitored as a function of time. The half-time of crystallization, $t_{1/2}$ (i.e., the time required for the material to reach 50% of its maximum crystallinity), was used as a quantitative comparison of the rate of bulk isothermal crystallization.

Results and Discussion

The experiments described in this paper were conducted to determine whether simple extrusion of montmorillonite clays with PBT-ionomers could result in the production of nanocomposites. All work described in this paper was done using either Na^+ montmorillonite or a commercially available organically modified montmorillonite clay (R_4N^+ montmorillonite) sold by Southern Clay Products under the trade name Claytone HY.

Morphology. The morphology of the nanocomposites of interest was determined using TEM and SAXS. Figure 3 shows the effect of organic modification of montmorillonite on the dispersed phase morphology of PBT composites. For a 95/5 wt/wt PBT/Na^+ montmorillonite composite, the Na^+ montmorillonite dispersed phase possessed many particles in the micron range when viewed in cross section, as shown in Figure 3A. The inability to observe individual silicate layers within the particles indicates that PBT did not exfoliate the Na^+ montmorillonite particles. When the cationic species of the montmorillonite was changed from Na^+ to R_4N^+, allowing for an increase in the interlayer distance and the production of a more organophillic environment at the surface of the platelets, a dramatic change in the morphology of the montmorillonite dispersed phase occurred, as shown in Figure 3B. The size of many of the R_4N^+ montmorillonite-derived particles are almost an order of magnitude smaller than the Na^+ montmorillonite particles, and the layered structure of the particles is discernible, suggesting some intercalation of PBT into the interplatelet galleries. A significant number of tactoids comprised of a few platelets were observed as well as some individual platelets; however, most of the R_4N^+ montmorillonite appeared to be intercalated structures with multiple platelets per particle.

The incorporation of 5.0 mol % $-SO_3Na$ groups into PBT had little effect on the morphology of Na^+ montmorillonite composites, as shown in Figure 4A. The features of the Na^+ montmorillonite particle morphology appear to be essentially the same as those of the analogous PBT/Na^+ montmorillonite composite (Figure 3A). For R_4N^+ montmorillonite-based composites, the presence of $-SO_3Na$ groups in the PBT dramatically changed the morphology of the montmorillonite-dispersed phase (Figure 4B). The morphology of a R_4N^+ montmorillonite nanocomposite derived from a PBT-SO_3Na matrix containing 5.0 mol % $-SO_3Na$ groups was found to consist exclusively of individual platelets and tactoids of the montmorillonite dispersed in the matrix. From the photomicrographs shown in Figure 5, it appeared that as little as 1.0 mol % $-SO_3Na$ groups in the matrix polymer resulted in virtually complete exfoliation. The particle size of the montmorillonite dispersed phase appeared to change very little, if at all, as the concentration of $-SO_3Na$ groups was increased from 1.0 to 5.0 mol %. To illustrate the decrease in particle size obtained by the introduction of $-SO_3Na$ groups into the PBT, the mean free path (MFP), which is the average 3-dimensional distance between particles calculated using commercially available imaging software, was determined. The smaller the MFP, the higher the particle density and thus the greater the degree of montmorillonite exfoliation. The MFP for the PBT/R_4N^+ montmorillonite and PBT-3.0% SO_3Na/R_4N^+ montmorillonite nanocomposites shown in Figure 5 was 68.4 and 33.4 nm, respectively.

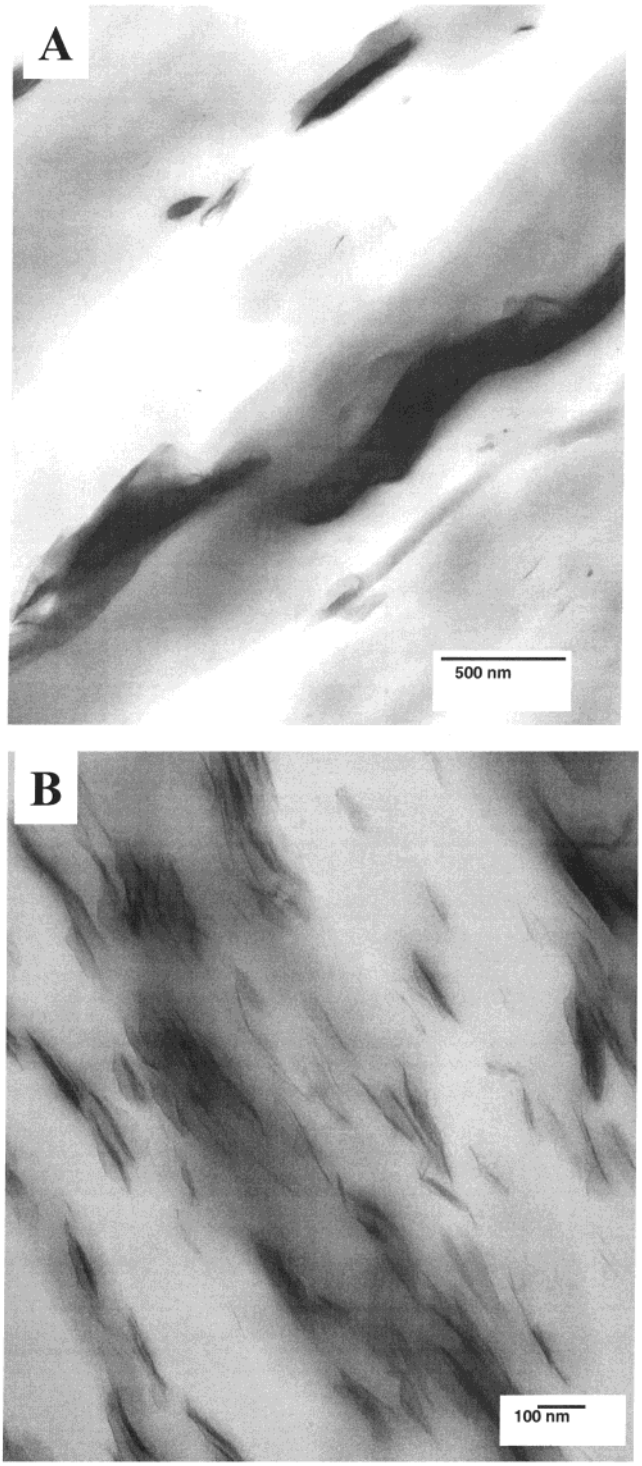

Figure 3. TEM micrographs of PBT composites: (A) PBT + 5% Na^+ montmorillonite; (B) PBT + 5% R_4N^+ montmorillonite.

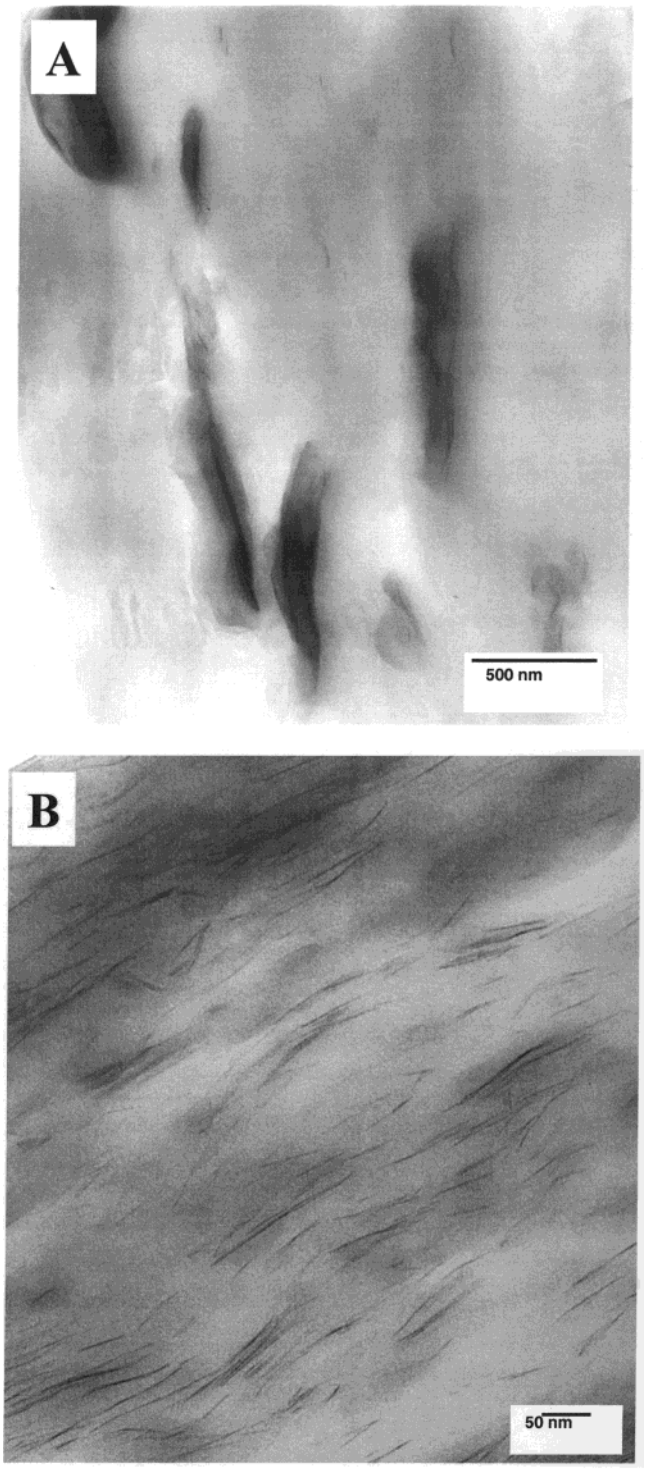

Figure 4. TEM micrographs of PBT-5.0% SO_3Na composites: (A) PBT-5.0% SO_3Na + 5% Na^+ montmorillonite; (B) PBT-5.0% SO_3Na + 5% R_4N^+ montmorillonite.

Figure 6 compares the SAXS data from the PBT and PBT-ionomer composites containing R_4N^+ montmorillonite. Within the range of scattering angles used in this study, intercalated structures should yield scattering peaks with a maximum in intensity corresponding (through the application of Bragg's law) to the average interlayer spacings of the silicate particle tactoids (multiplatelet aggregates).

The addition of R_4N^+ montmorillonite in the PBT matrix (Figure 6) yielded a scattering profile containing a distinct peak centered at 2.6° 2θ, corresponding to a Bragg spacing of d_{Bragg} = 3.40 nm. The pure Claytone HY (R_4N^+ montmorillonite), in the absence of a polymeric matrix, yielded a scattering maximum centered at 3.15° 2θ (d_{Bragg} = 2.8 nm). These data confirmed the TEM results that showed the R_4N^+ montmorillonite existing primarily as intercalated tactoids in the PBT matrix.

With the use of the PBT-ionomers, a pronounced decrease in the intensity of the scattering peak attributed to the intercalated morphology was observed. This behavior suggests that the clay tactoids are becoming homogeneously dispersed into individual platelets (i.e., exfoliation), which is in complete agreement with the TEM results for these samples. Moreover, this SAXS analysis in conjunction with the TEM analysis strongly suggests that the interfacially active PBT-ionomers yield strong specific interactions that permit the polymer chains to efficiently partition into the gallery spacings of the organically modified clay particles in order to disrupt the tactile interactions between platelets. With the application of significant shear during the melt extrusion process in this study, the separated platelets peel apart and become homogeneously dispersed in the PBT-ionomer matrix.[20]

In light of the charged surface characteristics of the montmorillonite clay particles (i.e., negatively charged gallery surfaces and positively charged edge surfaces), it is surprising and quite remarkable that a negatively charged ionomer is an effective exfoliation agent. A tentative model for the observed behavior, however, may be rationalized on the basis of recent studies of surfactant−clay interactions. Hild and co-workers[21] have shown that negatively charged sodium dodecylsulfonate (SDS) surfactants bind to the positively charged edge surface of sodium montmorillonite. In a similar fashion, it is reasonable to expect that the negatively charged, sulfonate groups along the ionomer chains first bind to the edges of the clay platelet tactoids. With this attachment of the polymer chains at the site of entrance to the galleries, it is likely that diffusion of mobile chain segments of the bound ionomer into the organically modified gallery spacings will be facilitated. This intercalation, driven by favorable enthalpic interactions between the organic modifier and the organic polymer chains, leads to a peeling apart of the individual clay platelets and ultimately exfoliation.[20,22] Furthermore, once the ionomer chains partition into the galleries, the low concentration of sodium sulfonate ion pairs along the ionomer chains may also interact with the platelet surfaces by dipole−dipole interactions. In contrast, while binding of the ionomer to the edges of pure sodium montmorillonite is also likely to occur, the lack of organic character in the gallery spacing inhibits intercalation, and thus no exfoliation is observed.

Favorable ionomer−clay interactions were also found to affect platelet orientation in injection-molded samples. All of the photomicrographs and SAXS data discussed above were generated from the material residing in the middle of an ASTM type IV tensile bar. Specimens for electron microscopy were taken as a cross section through the thickness (Z) direction. The mold used to produce the tensile specimens contained one gate, which was at one end of the mold. It was clear from the micrographs that a great deal of orientation of the montmorillonite occurred at this position of the specimen during injection molding. The montmorillonite particles were aligned parallel to the top and bottom

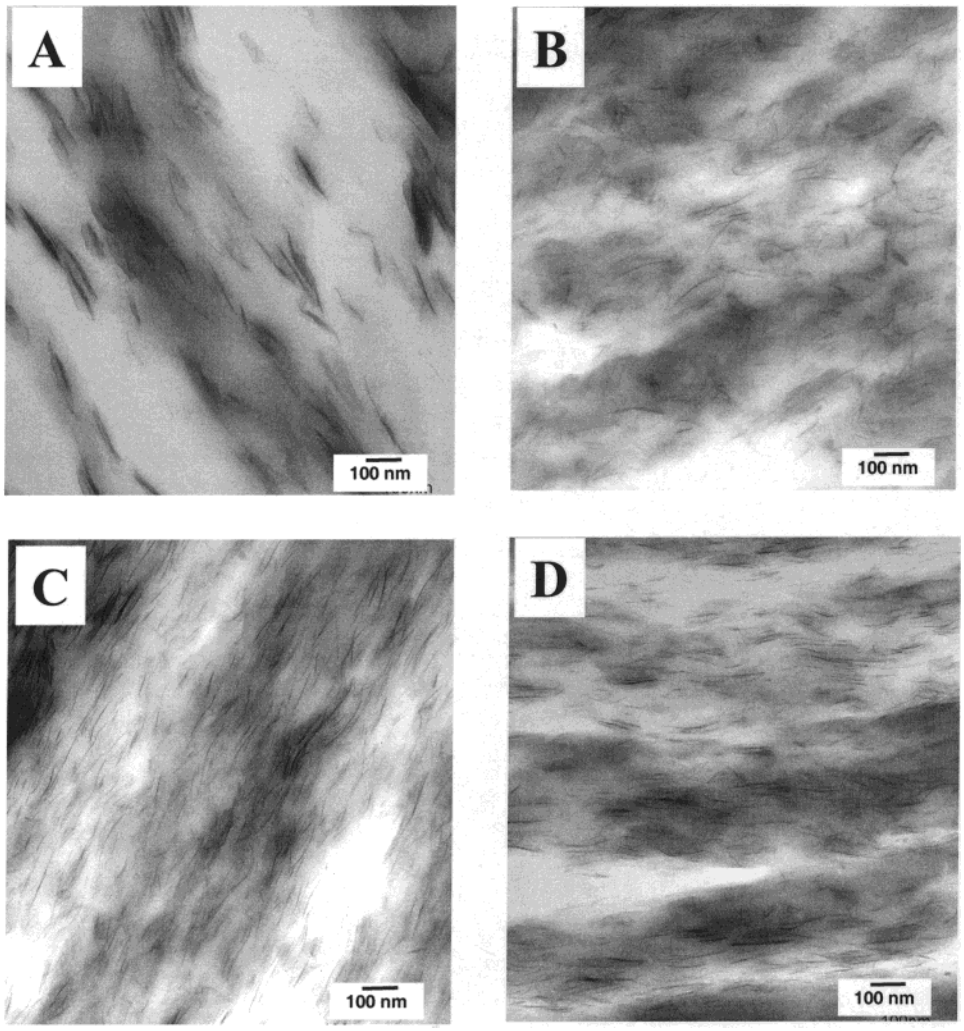

Figure 5. TEM micrographs of PBT-SO_3Na/ R_4N^+ montmorillonite composites of varying $-SO_3Na$ content: (A) 0 mol % SO_3Na; (B) 1.0 mol % SO_3Na; (C) 3.0 mol % SO_3Na; (D) 5.0 mol % SO_3Na.

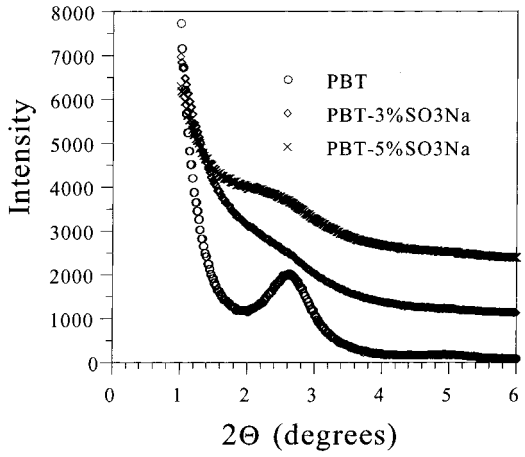

Figure 6. SAXS data from the PBT and PBT-ionomer composites containing R_4N^+ montmorillonite. Curves for the PBT-3.0% SO_3Na and PBT-5.0% SO_3Na nanocomposites are offset vertically by 1000 and 2000 intensity units, respectively.

surface of the tensile specimen such that the images produced exhibit primarily the thickness of the particles.

The degree of particle anisotropy was quantified using SAXS by directing the X-ray beam along the labeled *Z*-axis (i.e., through the sample cross section and parallel to the flow direction during the molding process), as shown in Figure 2. Using a 2-dimensional position-sensitive detector, 2-D scattering profiles were obtained for the purpose of evaluating the potential for preferential orientation of the clay platelets in the injected-molded samples. Figure 7 shows the intensity vs azimuthal angle plots (with the corresponding 2-D scattering profiles as insets) for the PBT, PBT-1.0% SO_3Na, PBT-3.0% SO_3Na, and PBT-5.0% SO_3Na samples containing 5 wt % R_4N^+ montmorillonite. For all of the samples, significant anisotropy was observed with a maximum intensity at an azimuthal angle of 90°. This scattering behavior was identical to that observed with injection-molded nylon-6−clay nanocomposites and indicated that the basal plane of the clay platelets was preferentially aligned parallel with the flat surface of the tensile specimen.[8,23] Similar platelet orientation has also been observed in thin films as well.[24,25] The 2-D SAXS data for the PBT/R_4N^+ montmorillonite sample (Figure 7) shows scattering behavior characteristic of an oriented lamellar structure with clear observation of the first- and second-order reflections. These data indicated that the clay in pure PBT was primarily in an intercalated morphology (in agreement with the TEM data in Figure 3) and that the multilayered tactoids were aligned in the flow direction.

With the introduction of the $-SO_3Na$ functionality in the PBT, the specific interactions facilitated exfoliation of the intercalated structures. This level of morphological disorder caused the elimination of higher-order

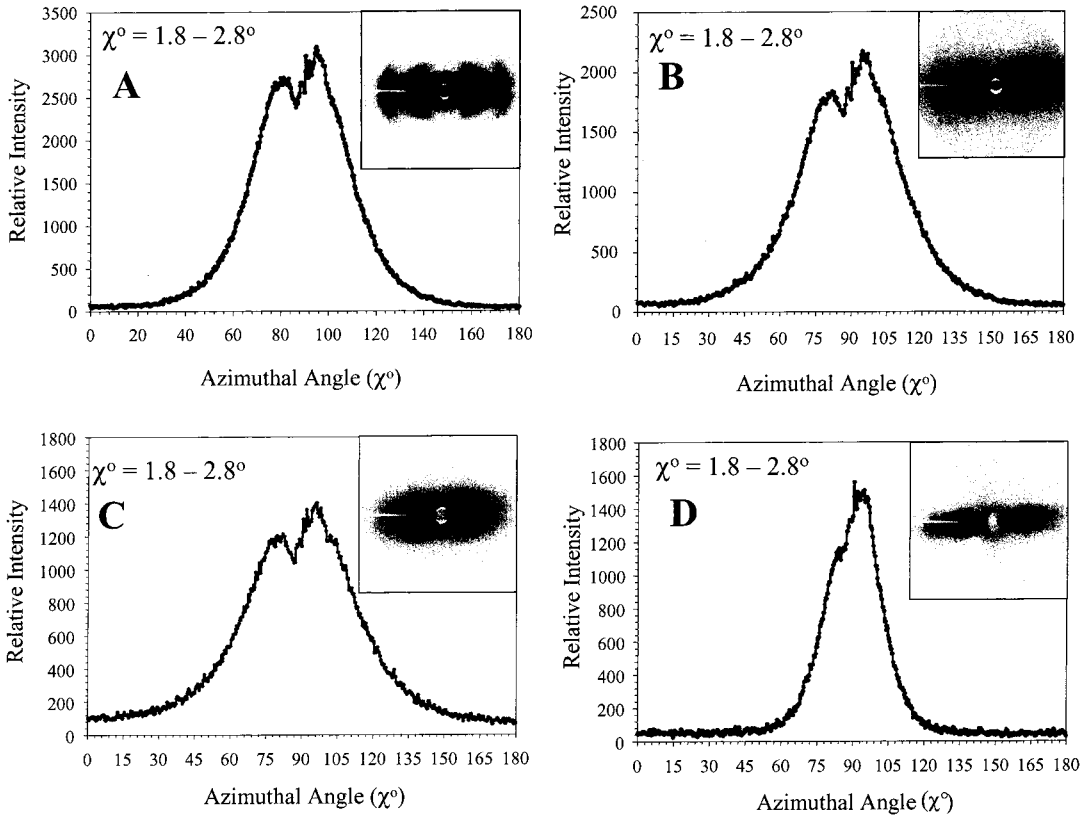

Figure 7. 2-D scattering profiles obtained for composites illustrating preferential orientation of the clay platelets in injected-molded samples as a function of $-SO_3Na$ content: (A) 0 mol % SO_3Na; (B) 1.0 mol % SO_3Na; (C) 3.0 mol % SO_3Na; (D) 5.0 mol % SO_3Na.

Table 1. Orientation Function Data

sample composition	full width at half-height (fwhh) (deg)[a]	orientation parameter Z = (fwhh/180)[b]
PBT/R_4N^+ montmorillonite	45	0.25
PBT-3%SO_3Na/R_4N^+ montmorillonite	52	0.29
PBT-5%SO_3Na/R_4N^+ montmorillonite	27	0.15

[a] Curves were peak fit utilizing Grams software. [b] Orientation parameter "Z" approaches 0 for maximum orientation and approaches 1 for random orientation.

reflections in the scattering profiles of the PBT-SO_3Na/R_4N^+ montmorillonite samples, seen in Figure 7. Moreover, as the ion content of the PBT-SO_3Na increased, the degree of platelet orientation in the injection-molded parts increased significantly. The most profound increase in orientation was observed with an increase in ion content from 3.0 to 5.0 mol % (see the orientation function data in Table 1). Therefore, it was reasonable to conclude that the strong specific interactions between the clay particle surfaces and the PBT-SO_3Na facilitated both exfoliation and the alignment of the platelets during melt flow in the injection-molding process. As the PBT-SO_3Na chains physically attached to the clay platelet surfaces via strong electrostatic interactions (specifically at the edges of the platelets), the platelets were more easily aligned with chain extension in the flow field.

Viscoelastic Properties. DMA was performed on injection-molded nanocomposites to determine the effect that organic modification of the montmorillonite and modification of the PBT by the incorporation of $-SO_3Na$ groups have on viscoelastic properties. To understand the viscoelastic properties of the nanocomposites, it was important to understand the viscoelastic properties of the polymer matrix materials. Parts A and B of Figure 8 display the tan δ and storage modulus (G') data obtained for the matrix polymers, respectively. The $-SO_3Na$ functionality resulted in a significant change in the tan δ vs temperature behavior of the polymer while very little effect was found for the G' vs temperature response. As shown in Figure 8A, the peak in the tan δ associated with the glass transition temperature (T_g) broadened with increasing $-SO_3Na$ content, and the temperature of the maximum of the transition increased with increasing $-SO_3Na$ content. This relationship between T_g and ionic content is typical for ionomers and is a consequence of the reduced mobility of the polymer backbone imparted by the strong electrostatic interactions between ionic groups.[26]

At temperatures above the T_g, tan δ increased with increasing $-SO_3Na$ content, indicating that the ionic groups resulted in greater mechanical energy dissipation over this temperature region. A reasonable explanation for this behavior may be that a second, high-temperature relaxation mechanism exists in the broad range of 130−160 °C that is attributed to the relaxation of chain segments located in a region of restricted mobility near the ionic aggregates.[27] This type of relaxation mechanism is commonly observed for ionomers and is referred to as a "cluster phase T_g". With an increase in the ionic content, more aggregates are formed, yielding a greater volume fraction of chains in the region of restricted mobility and, thus, a more pronounced relaxation (i.e., a greater tan δ response).

The observation that, above T_g, G' changed only slightly with $-SO_3Na$ content was somewhat surprising.

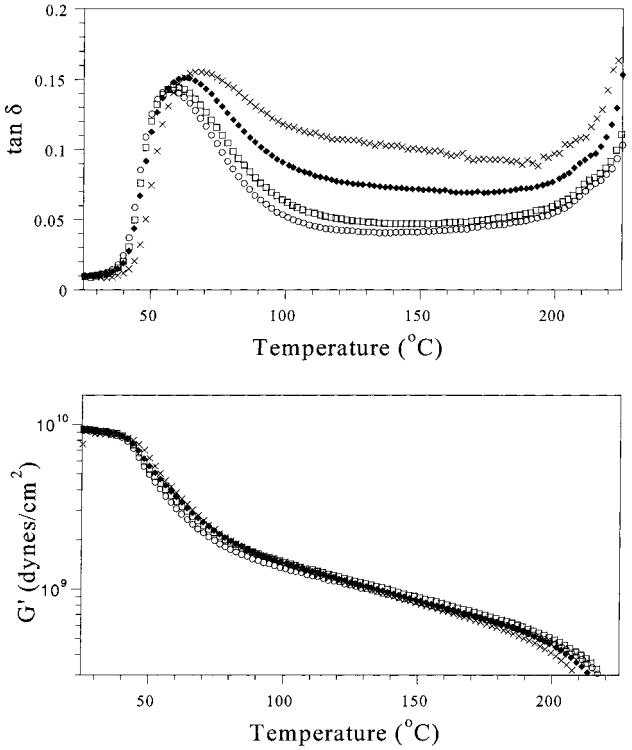

Figure 8. Tan δ and storage modulus (G') data obtained for the matrix polymers of interest: (○) PBT; (□) PBT-1.0% SO_3-Na; (◆)PBT-3.0% SO_3Na; (×) PBT-5.0% SO_3Na.

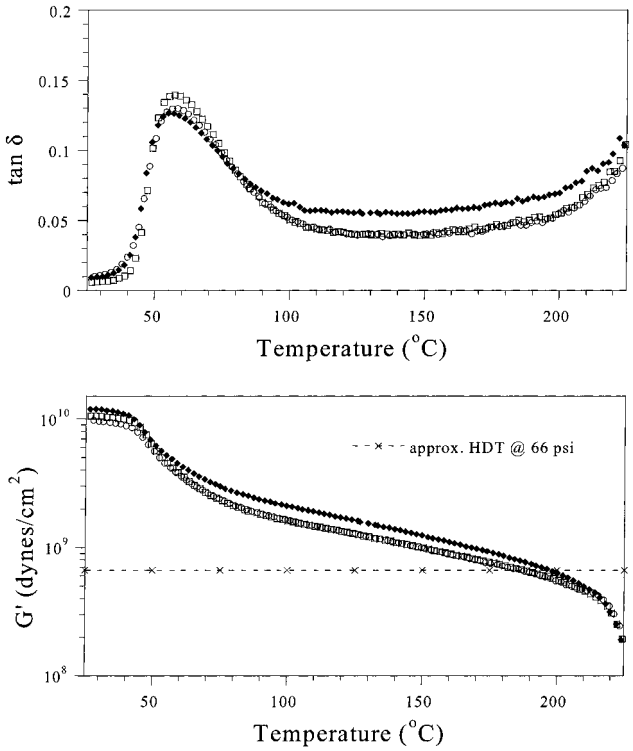

Figure 9. Tan δ and storage modulus (G') data obtained for PBT composites: (○) PBT; (□) PBT + Na + montmorillonite; (◆) PBT + R_4N^+ montmorillonite.

Typically, G' values at temperatures between T_g and the melting temperature depend on the degree of crystallinity and the crystalline morphology since the crystallites restrict polymer chain mobility and thus significantly contribute to the elastic response of the material.[26] For semicrystalline ionomers, the presence of the ionic groups typically results in a reduction in the rate of crystallization,[28] which would result in a reduction in crystallinity when specimens are produced by injection molding using similar conditions for all materials. Thus, a reduction in G' with increasing $-SO_3$-Na content would be expected on the basis of differences in crystallinity alone. Adversely, it has been shown for amorphous ionomers that the presence of ionic aggregates can result in the production of a G' plateau above T_g due to the ionic aggregates acting as transient cross-links.[26] Therefore, the presence of the ionic groups may have provided an enhancement in G' that compensated for any reductions due to decreased crystallinity.

The viscoelastic properties of composites comprised of PBT and Na^+ montmorillonite as well as PBT and R_4N^+ montmorillonite are shown in Figure 9. The presence of 5 wt % Na^+ montmorillonite had essentially no effect on the PBT T_g or the G' response with temperature, while the presence of 5 wt % R_4N^+ montmorillonite resulted in a marginal increase in G', especially at temperatures exceeding the PBT T_g. The increase in G' resulted from the smaller montmorillonite particle size obtained with the use of R_4N^+ montmorillonite as compared to Na^+ montmorillonite. The smaller montmorillonite particle size and corresponding larger particle surface area increased modulus by increasing the number of particle−matrix interactions.

As shown in Figure 10 for composites comprised of a PBT−ionomer matrix containing 5.0 mol % $-SO_3Na$ groups, the enhancement in G' obtained by adding Na^+ montmorillonite, or much more prominently, R_4N^+

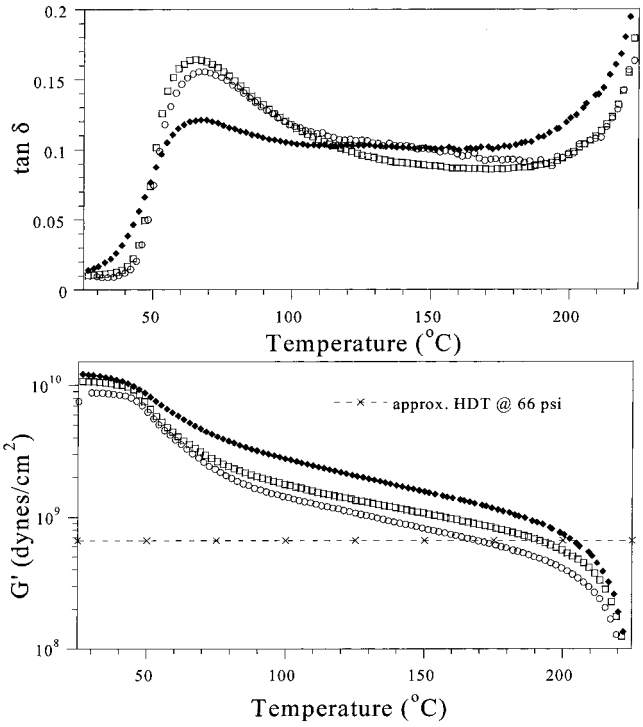

Figure 10. Tan δ and storage modulus (G') data obtained for PBT-5.0% SO_3Na composites: (○) PBT-5.0% SO_3Na; (□) PBT-5.0% SO_3Na + Na^+ montmorillonite; (◆) PBT-5.0% SO_3Na + R_4N^+ montmorillonite.

montmorillonite was much higher than in the absence of $-SO_3Na$ groups. For the PBT-5.0% SO_3Na/R_4N^+ montmorillonite composite, this result was attributed to the much greater exfoliation of this material as compared to the PBT Na^+/R_4N^+ montmorillonite.

For the PBT and PBT-ionomer systems, it is important to note that the magnitude of the tan δ peak

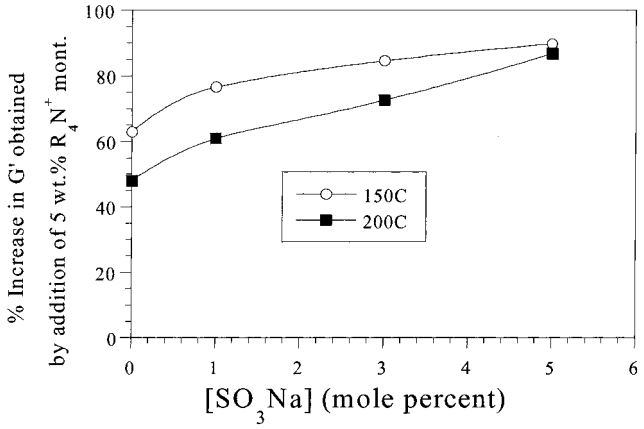

Figure 11. Increase in G' at 150 and 200 °C resulting from the addition of 5 wt % R_4N^+ montmorillonite.

attributed to the matrix T_g (at ca. 60 °C) decreases with the addition of R_4N^+ montmorillonite. Furthermore, this behavior is amplified with an increase in the $-SO_3Na$ content and is consistent with an increase in the quantity of chains residing in regions of restricted mobility. As the clay platelets become exfoliated, the high surface area of the nanoparticles and the strong specific interactions between the ionomer and the platelet surfaces result in a more efficient immobilization of the chains near the rigid clay particles. With a greater volume fraction of chains in regions of restricted mobility, fewer chains are available to contribute to the relaxation of the unperturbed matrix (i.e., the relaxation at $T_g = 60$ °C), and consequently more chains contribute to the high-temperature relaxation. Therefore, these DMA results clearly indicate that the PBT-ionomers interact more strongly with the R_4N^+ montmorillonite than the pure PBT matrix, and the exfoliated clay particles have a pronounced effect on the dynamic mechanical properties of the resulting nanocomposite.

With regard to the G' response as a function of $-SO_3Na$ content, G' at temperatures between the T_g and melting temperature increased as a result of the presence of $-SO_3Na$ groups; yet, little change was observed in the magnitude of G' when the $-SO_3Na$ content was increased from 1.0 to 5.0 mol % (Figure 8). In contrast, a significant increase in G' was observed as a result of the introduction of the R_4N^+ montmorillonite into the polymer matrix, and this behavior was found to increase with $-SO_3Na$ content, as shown in Figure 11. This G' behavior resulting from changes in $-SO_3Na$ content is most likely the result of the interplay between degree of clay exfoliation, degree of interaction between the matrix and clay particles, and the level of crystallinity. Increasing $-SO_3Na$ content may positively affect G' via an increase in the degree of clay exfoliation and an increase in the extent of interaction between the surface of the clay and the matrix, but G' is negatively affected by a decrease in the level of crystallinity resulting from an increase in $-SO_3Na$ content. Assuming the degree of clay exfoliation remains relatively constant with $-SO_3Na$ content from 1.0 to 5.0 mol %, as suggested by the TEM data, and the degree of crystallinity is largely unaffected by the presence of the clay particles, as suggested by the crystallization data presented in the final section of this report, then the G' behavior described by Figure 11 would therefore be due to an increasing degree of interaction between the matrix and dispersed phase with increasing $-SO_3Na$ content.

Table 2. Young's Modulus Data Obtained from Tensile Testing[a]

clay type	PBT	PBT-3% SO_3Na	PBT-5% SO_3Na
pure polymer	169000 ± 7500	165000 ± 7400	157000 ± 5800
Na^+ montmorillonite	182000 ± 50	178000 ± 5100	178000 ± 2000
R_4N^+ montmorillonite	196000 ± 3800	210000 ± 7300	215000 ± 7600

[a] The unit for all values is pounds per square inch.

Mechanical Properties. Tensile properties of the polymers and composites of interest were determined by measuring load or force as a function of crosshead displacement. Table 2 illustrates the effect of the addition of 50 wt % Na^+ montmorillonite or 5 wt % R_4N^+ montmorillonite had on the tensile properties of PBT, PBT-3.0% SO_3Na, and PBT-5.0% SO_3Na. All materials were compounded and injection-molded side-by-side. None of the materials based on PBT-3.0% SO_3Na or PBT-5.0% SO_3Na exhibited consistent yielding, while the PBT and PBT/Na^+ montmorillonite composite showed yielding. The lack of a yield point for PBT-3.0% SO_3Na and PBT-5.0% SO_3Na as well as for the clay composites derived from these polymers may be due to the relatively low molecular weight of these polymers as compared to the PBT.[18] The experiments described in this document were designed to compare materials at similar melt viscosity. Since the presence of the $-SO_3Na$ groups result in an increase in melt viscosity due to the reduction in molecular mobility imparted by ionic interactions, it was necessary to utilize PBT-SO_3Na polymers of lower molecular weight to offset the ionically induced viscosity increase. Apparently, the PBT-SO_3Na polymers were low enough in molecular weight that a sufficient degree of chain entanglement to support yielding was not achieved.

Table 2 shows that, for all polymers, the addition of R_4N^+ montmorillonite provided a larger increase in Young's modulus than an equivalent addition of Na^+ montmorillonite. In addition, the presence of $-SO_3Na$ groups in the PBT resulted in a further increase in Young's modulus with the magnitude of the enhancement increasing as the $-SO_3Na$ content increased from 3.0 to 5.0 mol %. It is important to note here that a recent study by Matayabas and Turner has shown that montmorillonite clay can severely degrade the molecular weight of polyesters during melt extrusion.[29] While this molecular weight degradation is likely to have occurred in these PBTI samples as well, the data shown in Table 2 indicate significant improvements in modulus with added clay. Thus, the reinforcing effect of the nanoparticles apparently offsets, to some degree, an undesirable deterioration of this mechanical property that would be expected from degradation in molecular weight.

The higher Young's modulus obtained with the use of R_4N^+ montmorillonite as compared to Na^+ montmorillonite was attributed to the smaller montmorillonite particle size obtained with the former. A smaller particle size translates to a greater clay surface area and thus the opportunity for a larger number of interactions between the polymer molecules and the montmorillonite. As a result, higher stresses are required to cause elastic deformation of the composite.

Crystallization. Some inorganic fillers such as talc have been shown to be nucleating agents for the crystallization of polyesters such as PBT and poly(ethylene terephthalate).[30,31] As a result, it was of interest to investigate the effect of R_4N^+ montmorillo-

Table 3. Isothermal Crystallization Half-Times $t_{1/2}$ (min)

mol % SO_3Na	0	1.0	3.0	5.0
pure polymer	4.81	7.33	11.13	17.46
Na^+ montmorillonite	5.35		17.12	18.11
R_4N^+ montmorillonite	6.04	8.23	14.38	19.95

nite and Na^+ montmorillonite on the crystallization rate of PBT and the PBT-ionomers. To determine the effect of the presence of the montmorillonite particles on crystallization rate, it was necessary as well as other polyesters and polyamides that all materials including pure PBT and the pure PBT-ionomers be melt-processed in the same fashion. This requirement is due to the "melt memory" effect observed for PBT.[31,32] With this phenomenon in mind, the samples used for investigating crystallization rate were melt-processed using identical processing conditions, and the samples were cut from the same location of injection-molded tensile specimens. A convenient and reproducible method for comparing the crystallization rate of polymer samples with the same equilibrium melting temperature is to compare the time required to reach 50% crystallinity during isothermal crystallization. With this type of comparison, the longer the crystallization half-time, the slower the overall rate of bulk crystallization.

Table 3 lists the crystallization half-time, $t_{1/2}$, of the crystallization isotherms for PBT, PBT-1.0% SO_3Na, PBT-3.0% SO_3Na, and PBT-5.0% SO_3Na-containing materials. From these data, neither Na^+ montmorillonite nor R_4N^+ montmorillonite enhanced the rate of crystallization of PBT or any of the PBT-ionomers. In fact, the addition of clay slightly decreased the rate of crystallization for all samples. This behavior is in contrast to that observed for poly(ethylene terephthalate)-based nanocomposites.[22,33] This observation suggests that clay particles are not effective nucleating agents for PBT crystallization, and the decrease in crystallization rate may be attributed to an increase in the viscosity of the melt.

Conclusions

The results of this study clearly show that organic modification of montmorillonite clay coupled with the modification of PBT with low levels (1.0−5.0 mol %) of $-SO_3Na$ groups results in the production of nanocomposites by a simple extrusion process. With regard to the effect of $-SO_3Na$ content, as little as 1.0 mol % $-SO_3Na$ groups was needed to achieve considerable exfoliation of R_4N^+ montmorillonite. A tentative model for the influence of ionic groups on exfoliation is rationalized and based on ionic interactions between the negatively charged ionomer and the positively charged edge surfaces of the montmorillonite clay platelets. With attachment of the polymer chains at the site of entrance to the galleries, diffusion of mobile chain segments of the bound ionomer into the organically modified gallery spacings is likely to be facilitated. This intercalation, driven by favorable enthalpic interactions between the organic modifier and the organic polymer chains, leads to a peeling apart of the individual clay platelets and ultimately exfoliation.

Although the degree of exfoliation was not observed to be strongly dependent on $-SO_3Na$ content, mechanical properties and clay platelet orientation were found to depend on $-SO_3Na$ content. Young's modulus increased with increasing $-SO_3Na$ content, and the enhancement in storage moduli at temperatures above T_g obtained by the addition of R_4N^+ montmorillonite increased with increasing $-SO_3Na$ content. These enhancements in mechanical properties produced by a higher $-SO_3Na$ content were believed to be due to an increase in the number of interactions between the clay particles and the matrix via strong specific interactions involving the $-SO_3Na$ groups. A higher number of matrix/clay interactions would require greater stresses to strain the material. In addition, clay platelet orientation increased with increasing $-SO_3Na$ content which further suggests the presence of strong matrix/clay interactions.

References and Notes

(1) Zanetti, M.; Lomakin, S.; Camino, G. *Macromol. Mater. Eng.* **2000**, *279*, 1.
(2) Krishnamoorti, R.; Vaia, R. A.; Giannelis, E. P. *Chem. Mater.* **1996**, *8*, 1728.
(3) Giannelis, E. P. *Adv. Mater.* **1996**, *8*, 29.
(4) Alexandre, M.; Dubois, P. *Mater. Sci. Eng.* **2000**, *28*, 1.
(5) Fukushima, Y.; Inagaki, S. *J. Inclusion Phenom.* **1987**, *5*, 473.
(6) Usuki, A.; Kojima, Y.; Kawasumi, M.; Fukushima, Y.; Kurauchi, T.; Kamigaito, O. *J. Mater. Res.* **1993**, *8*, 1179.
(7) Kojima, Y.; Usuki, A.; Kawasumi, M.; Okada, A.; Fukushima, Y.; Kurauchi, T.; Kamigaito, O. *J. Mater. Res.* **1993**, *8*, 1185.
(8) Varlot, K.; Reynaud, E.; Kloppfer, M. H.; Vigier, G.; Varlet, J. *J. Polym. Sci., Part B: Polym. Phys.* **2001**, *39*, 1360.
(9) Lan, T.; Kaviratna, P. D.; Pinnavaia, T. J. *Chem. Mater.* **1994**, *6*, 573.
(10) Krishnamoorti, R.; Giannelis, E. P. *Macromolecules* **1997**, *30*, 4097.
(11) Kojima, Y.; Usuki, A.; Kawasumi, M.; Okada, A.; Kurauchi, T.; Kamigaito, O. *J. Polym. Sci., Part A: Polym. Chem.* **1993**, *31*, 1755.
(12) Kornmann, X.; Berglund, L. A.; Sterte, J.; Giannelis, E. P. *Polym. Eng. Sci.* **1998**, *38*, 1351.
(13) Kornmann, X.; Lindberg, H.; Berglund, L. A. *Polymer* **2001**, *42*, 4493.
(14) Kaviratna, P. D.; Lan, T.; Pinnavaia, T. J. *Polym. Prepr. (Am. Chem. Soc., Polym. Div.)* **1994**, *35*, 788.
(15) Zilg, C.; Mulhaupt, R.; Finter, J. *Macromol. Chem. Phys.* **1999**, *200*, 661.
(16) Burnside, S. D.; Giannelis, E. P. *Chem. Mater.* **1995**, *7*, 1597.
(17) Takeuchi, H.; Cohen, C. *Macromolecules* **1999**, *32*, 6792.
(18) Chisholm, B. J.; Richards, W.; Banach, T.; Soloveichik, S.; Eddy-Helenek, V.; Bradtke, G.; Kelley, J. Manuscript in preparation.
(19) Gorda, K. R.; Peiffer, D. G. *J. Polym. Sci., Polym. Phys. Ed.* **1992**, *30*, 281.
(20) Dennis, H. R.; Hunter, D. L.; Chang, D.; Kim, S.; White, J. L.; Cho, J. W.; Paul, D. R. *Polymer* **2001**, *42*, 9513.
(21) Hild, A.; Sequaris, J.-M.; Narres, H. D.; Schwuger, M. J. *Prog. Colloid Polym. Sci.* **1833**, *111*, 174.
(22) Ke, Y.; Long, C.; Qi, Z. *J. Appl. Polym. Sci.* **1999**, *71*, 1139.
(23) Kojima, Y.; Usuki, A.; Kawasumi, M.; Okada, A.; Kurauchi, T.; Kamigaito, O.; Kaji, K. *J. Polym. Sci., Part B: Polym. Phys.* **1995**, *33*, 1039.
(24) Jimenez, G.; Ogata, N.; Kawai, H.; Ogihara, T. *J. Appl. Polym. Sci.* **1997**, *64*, 2211.
(25) Kojima, Y.; Usuki, A.; Kawasumi, M.; Okada, A.; Kurauchi, T.; Kamigaito, O.; Kaji, K. *J. Polym. Sci., Part B: Polym. Phys.* **1994**, *32*, 625.
(26) Eisenberg, A.; King, M. *Ion-Containing Polymers: Physical Properties and Structure*; Academic Press: New York, 1977.
(27) Eisenberg, A.; Hird, B.; Moore, R. B. *Macromolecules* **1990**, *23*, 4098.
(28) Orler, E. B.; Calhoun, B. H.; Moore, R. B. *Macromolecules* **1996**, *29*, 5965.
(29) Matayabas, J. C.; Turner, S. R. In *Polymer-Clay Nanocomposites*; Pinnavaia, T. J., Beall, G. W., Eds.; John Wiley & Sons: New York, 2000; pp 207−226.
(30) Chisholm, B. J.; Fong, P. M.; Zimmer, J. G.; Hendrix, R. *J. Appl. Polym. Sci.* **1999**, *74*, 889.
(31) Chisholm, B. J.; Zimmer, J. G. *J. Appl. Polym. Sci.* **2000**, *76*, 1296.
(32) Khanna, Y. P.; Kumar, R.; Reimschussel, A. C. *Polym. Eng. Sci.* **1988**, *28*, 1612.
(33) Barber, G. D.; Moore, R. B. *Polym. Mater. Sci. Eng.* **2000**, *82*, 241.

MA012224N